American Mineralogist, Volume 72, pages 1195–1203, 1987

X-ray diffraction and ^{29}Si magic-angle-spinning NMR of opals: Incoherent long- and short-range order in opal-CT

B.H.W.S. DE JONG

Applied Physics, SP-DV-025, Corning Glass Works, Corning, New York 14831, U.S.A.

J. VAN HOEK, W. S. VEEMAN

Department of Physical Chemistry, University of Nijmegen, Toernooiveld, 6525 ED, Nijmegen, The Netherlands

D. V. MANSON

Gemmological Institute of America, 1660 Stewart Street, Santa Monica, California 90404, U.S.A.

Dedicated to Dr. J.G.Y. de Jong on his 78th birthday

ABSTRACT

X-ray diffraction and ^{29}Si MAS NMR experiments have been carried out to assess the structure of amorphous and quasi-crystalline natural and synthetic opals. We collected ^{29}Si MAS NMR spectra for nine opals, which, according to their X-ray signature, belong to either category A (amorphous) or CT (cristobalite-tridymite). All NMR spectra of natural opals have chemical shifts of about −112 ppm, characteristic of amorphous silica, and resemble in peak shape amorphous silica most and, for different reasons, silica gel and quartz least. The full width at half maximum (FWHM) of the NMR spectra increases in the order opal-CT, opal-A, and amorphous silica. None of the opal NMR spectra can be mimicked by combining those of the crystalline-silica polymorphs. Comparisons between X-ray and ^{29}Si MAS NMR spectra indicate that long-range order suggestive of cristobalite-tridymite intergrowth is not strongly coupled to short-range ordering. There is a distinct difference in ^{29}Si chemical shift between the eight natural opals and the synthetic one. Synthetic opal has a maximum chemical-shift peak intensity at −107.0 ppm, close to that for quartz (−107.4 ppm), in contrast to natural opals, whose maximum chemical-shift peak intensity is around −112 ppm, close to the average chemical-shift value of tridymite (−111.0). Because of this quartz-like character, synthetic opal has a higher density and refractive index in comparison to natural samples. It is an important characteristic of NMR spectroscopy that it can distinguish between amorphous substances with similar X-ray patterns.

INTRODUCTION

Nucleation is the principal process variable in the tectogenesis—i.e., the creation of structure—of crystalline compounds from amorphous starting materials. A facet in this process is the interaction between short- and long-range ordering. We shall address in the following this facet using opals as example.

Opal consists of 1500- to 3000-Å spheres of silica, mono- or polydisperse depending on the number of nucleation events, and occurs in a wide variety of natural settings (Frondel, 1962; Iler, 1979; Gauthier, 1985; Sanders, 1985; Deelman, 1986). X-ray diffraction experiments on natural opal from sedimentary basins reveal the occurrence of solid-state transitions from amorphous to crystalline, the various stages being designated opal-A (amorphous), opal-C (cristobalite), and opal-CT (cristobalite-tridymite). The final stage of burial metamorphism is indicated by the presence of quartz in opals. Thus opal and its various transition stages function as stratigraphic markers in sedimentary basins (Flörke, 1956; Murata and Nakata, 1974; Kastner, 1979; Kano, 1983; Graetsch et al., 1985, 1987).

Because X-ray diffraction of opal can only distinguish three stages, it seemed likely to us that additional stages in the solid-state transition between amorphous and crystalline opal could show up as variations in local Si environments. Such variations can be characterized by ^{29}Si MAS NMR, and thus a road seemed to open up toward a refined stratigraphic marker in sedimentary basins. In addition, study of opals in their various transition stages might shed some light on the nature of amorphous solids and the relation between amorphous-crystalline pairs, a subject that currently is receiving increasing attention (Phillips, 1980; Matson et al., 1983; Grimmer et al., 1984; de Jong et al., 1981, 1984a, 1984b; Gerstein and Nicol, 1985; Engelhardt et al., 1985; Gladden et al., 1986).

In this paper we show that in the opal-A to opal-CT transition, long-range order as determined by X-ray diffraction occurs first followed by short-range order, as determined by ^{29}Si MAS NMR. In addition, we show that all

0003–004X/87/1112–1195$02.00

opal-A and opal-CT samples used in this study show local Si environment distributions closely akin to those found in amorphous silica. Next, we show that the ^{29}Si MAS NMR spectra of opals cannot be constructed by simple superposition of the spectra of cristobalite and tridymite. Hereafter, we show that silica in opal is completely polymerized and that there is a fairly narrow range of Si–O–Si angles between those of amorphous silica and tridymite. Finally, we suggest reasons why long-range ordering and short-range ordering are not developed synchronously with one another.

Experimental details

Eight opals from different localities and one synthetic one were characterized by X-ray diffraction, chemical analysis, ESR, and proton and ^{29}Si magic-angle-spinning NMR. H_2O measurements on the samples were carried out in three temperature steps using a modified Karl-Fischer assaying method.

^{29}Si MAS NMR spectra were collected on a home-built spectrometer with a 4.2-T wide-bore Oxford magnet at 35 756 kHz and on a CXP 300 Bruker spectrometer at 59 600 kHz. Normal FT-NMR techniques in conjunction with MAS were used to obtain all spectra. Most spectra were collected without proton decoupling once it was observed that such decoupling did not affect the ^{29}Si line width nor line position in opals. Cylindrical rotors (8-mm internal diameter) were used for collection of the ^{29}Si MAS NMR spectra with typical spinning speeds of 2.5 kHz. A 90° pulse, varying recycle delay between 1 s and 1 h (30 s for the spectra discussed here), 1000 data points, and 20-kHz spectral line width were used in all cases. Line broadening due to exponential multiplication of the free-induction decay is 10 Hz. The ^{29}Si chemical shifts reported in this paper are referenced by sample exchange to TMS. Two spectra were run with benitoite (−94 ppm) as an internal standard (de Jong et al., 1984a).

Proton MAS NMR spectra were collected in similar fashion. Due to the much shorter proton T_1 relaxation time, recycle delays of 1 s were used. The proton spectra were referenced by sample exchange to benzene. The negative sign indicates that the protons in opals are more shielded than those in benzene. Proton and ^{29}Si MAS NMR spectra of one sample were measured after heat treatment for 24 h at 300 °C under vacuum (0.005-mm Hg). ESR spectra on opals were collected on a Varian E-123 (*x*-band) spectrometer at room temperature.

Density and refractive-index measurements were carried out using a picnometer and refractometer, respectively.

Results

Results of our X-ray diffraction and MAS NMR experiments are collected in Table 1 and illustrated in Figures 1, 2, 3, and 4. The opals in Table 1 are designated either opal-A or opal-CT depending on their amorphous or quasi-crystalline character as determined by X-ray diffraction (Fig. 3). The d_{011} spacing of cristobalite and tridymite are 4.05 and 4.10 Å, respectively. Larger d spacings are thought to be a measure of the tridymite-cristobalite transition in opal-CT (Kano, 1983). The d_{011} spacing in samples 2, 3, and 7 is 4.07, 4.13, and 4.11 Å, respectively, suggesting that sample 2 is most and sample 3 least like cristobalite. One sample, number 6, has an opal-A pattern with some quartz. The amorphous haloes of natural and synthetic opal-A have an intensity maximum at a 2θ of 22° (d_{avg} = 4.04 Å) and 21.5° (d_{avg} = 4.13 Å), respectively, slightly different and narrower than that of vitreous silica at a 2θ of 21° (d_{avg} = 4.23 Å).

Procedures for manufacturing synthetic opals have been developed by K. Inamori and P. Gilson. X-ray patterns of these synthetic opals, designated Inamori or Gilson opal, show the presence of ZrO_2, particularly in the Gilson opal as noted by other workers (Simonton et al., 1986; Gauthier, 1986). The calculated crystallite size of opal-CT, based on line broadening of the (011) diffraction line, varies between 60 and 90 Å, bracketing the c dimension of tridymite PO (81.864 Å) (Klug and Alexander, 1954; Fagherazzi et al., 1981; Konnert and Appleman, 1978; Vieillard, 1986; Nukui and Flörke, 1987).

The ^{29}Si chemical shifts of all natural opals fall around −112 ppm (Fig. 1), between the chemical shifts for cristobalite and tridymite. The full width at half maximum (FWHM) of ^{29}Si NMR peaks varies between 5.8 and 9.8 ppm for natural opals, but is substantially broader, 11 ppm, for the one synthetic sample. The ^{29}Si chemical shift of this sample is less negative, −107 ppm, and closer to the chemical shift of quartz, than those of the natural samples.

There are large variations in T_1 relaxation times for silica species. T_1 for quartz is of the order of 5 h, whereas T_1 for opals varies between 0.25 and 10 s, presumably because of the presence of either paramagnetic impurities or water in the latter (Gladden et al., 1986). The width of the components building up a ^{29}Si resonance line in opal is 50 Hz (1 ppm) as revealed by T_2 determinations obtained using the Hahn spin-echo technique (Hahn, 1950). The meaning of this result is that 50 Hz is the lower resolution limit between a collection of silica species and hence that the width of the ^{29}Si MAS NMR lines in opals is due to a distribution of silica species rather than to variations in relaxation effects.

Proton chemical shifts do not show large variations between samples. Proton decoupling does not affect the ^{29}Si spectral-line width nor its position. The water content, characteristic for physisorbed (20–105 °C) and chemisorbed (105–500 °C) water, varies between samples without discernible trend.

The ESR spectra were collected to determine if paramagnetic centers affect the opal NMR line width. Some samples (notably 3, 6, and 8) show strong ESR signals, indicative of substantial concentrations of paramagnetic centers, whereas others (samples 1, 4, and 5) do not. There is no significant difference in NMR line width between samples with high or low concentrations of paramagnetic centers (Table 1).

Discussion

Since the pioneering study of Lippmaa et al. (1980), ^{29}Si MAS NMR spectroscopy has become a well-established technique to probe the structure of crystalline aluminosilicates, particularly zeolites (Klinowski, 1984; Oldfield and Kirkpatrick, 1984; Kirkpatrick et al., 1985). On the

other hand, ^{29}Si MAS NMR experiments on silicate glasses are still fairly rare, though the number of such studies is rapidly increasing (Grimmer et al., 1984; de Jong et al., 1983, 1984a, 1984b; Murdoch et al., 1985; Dupree et al., 1984, 1986; Weeding et al., 1985; Fujiu and Ogino, 1984; Gerstein and Nicol, 1985; Engelhardt et al., 1985; Gladden et al., 1986; Kirkpatrick et al., 1986; Aujla et al., 1986; Yang et al., 1986; de Jong and Veeman, 1986; Devine et al., 1987; Turner et al., 1987; Schneider et al., 1987). Still unique is the NMR study on molten silicates of Stebbins et al. (1985).

We start our discussion with the ^{29}Si MAS NMR results for opals and compare these results with those for silica gel and glass. Next we discuss differences between the X-ray diffraction and MAS NMR results.

Comparison between ^{29}Si MAS NMR spectra of opals, silica gel, and silica glass

The ^{29}Si MAS NMR spectra of opals cover the chemical shift range of −99 and −123 ppm (Fig. 1). This range indicates that within NMR detection limits, all Si atoms are coordinated to four oxygens in a three-dimensional array of corner-sharing tetrahedra. Thus the uncommon configurations postulated by various authors to exist in amorphous silica, such as edge-sharing tetrahedra or threefold-coordinated Si (chemical shift less negative than 60 ppm), and fivefold- or sixfold-coordinated Si (chemical shift more negative than 130 ppm), if present, do not occur in sufficient concentrations in opal to be detected (O'Keeffe and Gibbs, 1984; Garofalini, 1984; Weyl and Marboe, 1959). The absence of silanol groups, i.e., Q_0, Q_1, Q_2, and Q_3 tetrahedra with protons attached to the nonbridging oxygens, is confirmed by the lack of line narrowing of the Si spectrum on proton decoupling, in accordance with the H_2O chemical analyses, which indicate

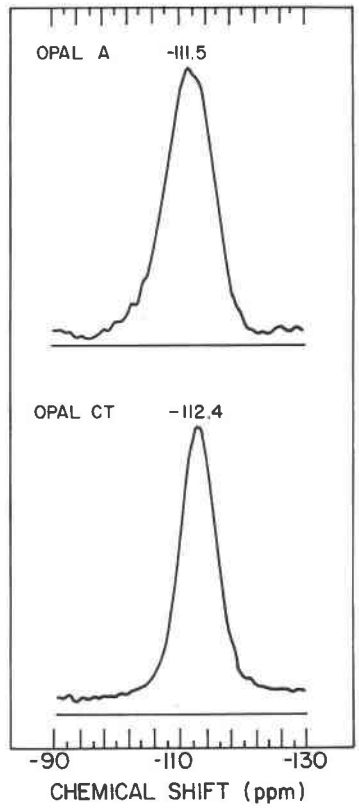

Fig. 1. ^{29}Si MAS NMR spectra of amorphous (opal-A) and quasi-crystalline (opal-CT) gem-quality opals.

that most water in these compounds is either physisorbed or chemisorbed, albeit that the second temperature step, 500 °C, is somewhat high for chemisorbed water, as pointed out by Knauth and Epstein, 1982. A fairly strong

TABLE 1. Proton and ^{29}Si chemical shifts, full width at half maximum (FWHM), number of Si free-induction decays (FID), and weight percent water in opals in temperature steps

Sample	Description	^{29}Si shift* (ppm)	^{1}H shift** (ppm)	FWHM (ppm)	FID	H_2O (wt%) 20–105 °C	105–500 °C	500–1000 °C
1	Opal-A	−111.8	−1.8	9.8	5009	n.d.	n.d.	n.d.
2	Opal-CT	−111.9	−1.7	6.2	5340	1.74	7.0	0.01
3	Opal-CT	−112.4	−1.7	5.8	8502	0.58	4.4	3.8
4	Opal-A	−111.5	−1.8	8.6	5650	n.d.	n.d.	n.d.
5	Opal-A	−111.5	−1.9	8.0	13592	2.04	4.6	0.27
6	Opal-A + qtz	−111.4	−1.7	9.8	2772	2.04	2.9	0.24
7	Opal-CT	−111.8	−1.8	7.2	7940	1.08	7.5	0.23
8	Opal-A	−111.5	−1.9	8.6	10658	2.68	4.1	0.01
9†	Opal-A + qtz	−110.6	n.d.	9.8	11188	2.04	2.9	0.24
10†	Opal-A + qtz	−111.9	—	10.6	6274	n.d.	n.d.	n.d.
11†	Opal-A + qtz	−111.4	n.d.	10.1	82	2.04	2.9	0.24
12	Opal-A‡	−107.0	n.d.	11.0	2500	n.d.	n.d.	n.d.

* Relative to TMS, proton shifts relative to TMS: benzene, 7.3 ppm; H_2O, 4.8–4.7 ppm; ⟨H⟩ in opal, 5.5 ppm.

** Relative to benzene.

† Three other experiments were carried out on sample 6: in sample 9, protons were decoupled; in sample 10, protons were removed after 24-h heat treatment at 300 °C; in sample 11, experiment was carried out on Bruker CXP 300 at 7.1 T.

‡ Inamori synthetic opal.

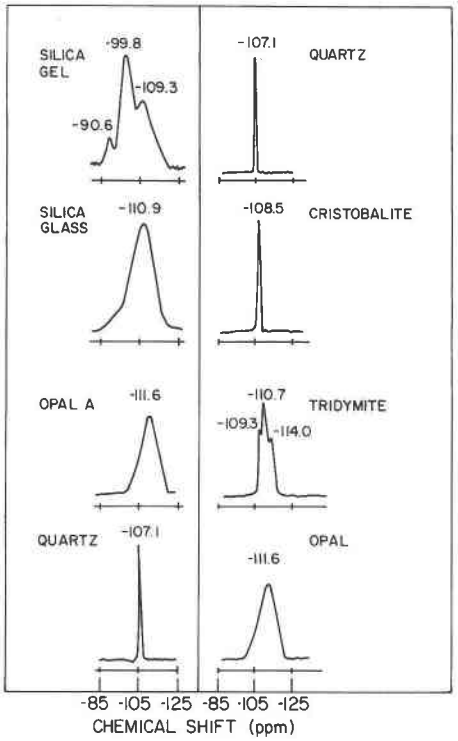

Fig. 2. ^{29}Si MAS NMR spectra of silica gel (Maciel and Sindorf, 1980), silica glass (Murdoch et al., 1985), quartz, tridymite (Smith and Blackwell, 1983), and opal.

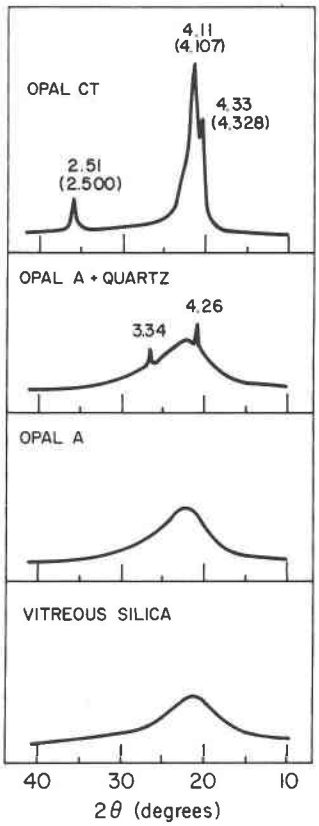

Fig. 3. X-ray diffraction patterns of opal-CT, opal-A + quartz, opal-A, and vitreous silica. The numbers in parentheses are the d spacings of tridymite.

interaction between water and silica is suggested by the observation that proton chemical shifts of opal are about 1.1 ppm more positive than for water (Table 1). This conclusion concerning the absence of silanol groups in opals differs from the one reached by Graetsch et al. (1985) based on IR data of opal-C.

Line broadening of the ^{29}Si MAS NMR spectra of opals may be caused by dipolar coupling between protons and ^{29}Si nuclei. To test for this possibility we carried out three additional NMR experiments on one sample (no. 6), in which the protons were decoupled (sample 9, Table 1), the spectrum was measured after removal of water (sample 10), and the spectrum was measured at 7.1 T rather than the standard 4.2 T (sample 11). The results in Table 1 indicate that the FWHM of the ^{29}Si spectra were not affected in these three experiments. Hence, the cause for the broad FWHM of opal-A spectra has to be found in a distribution of chemical shifts.

Of all the silica spectra considered here, the opal spectral shape resembles that of silica glass most and that of either silica gel or quartz least (Fig. 2). The differences between the spectra of silica glass and opal are that the peak maximum for opal is more negative [about -112 vs. -111.5 ppm (Gladden et al., 1986) or -110.9 ppm (Murdoch et al., 1985)] and that the FWHM for opal is smaller (5.6 to 9.8, vs. 11.6 ppm).

The distribution of mean Si–O–Si angles per tetrahedron, ⟨Si–O–Si⟩, for natural opals, calculated using the method of Thomas et al. (1983) and illustrated in Figures 4 and 5, indicates a narrower range for the opals than for silica glass. For opal-A, ⟨Si–O–Si⟩ varies between 133° and 168° with a maximum around 151°. For opal-CT, ⟨Si–O–Si⟩ varies between 138° and 170° with a maximum around 152°, whereas for silica glass, the range varies between 122° and 170° with a maximum around 148°. The ⟨Si–O–Si⟩ variation of the silica glass of Dupree and Pettifer (1984) indicates their sample to be most likely a gel. It should be noted that the calculation of ⟨Si–O–Si⟩ angles assumes that ^{29}Si chemical shifts of crystals and glasses correspond to one another, an assertion that, as we have demonstrated elsewhere (de Jong et al., 1984b), is not necessarily correct. It necessitates in addition that spectral-line width is caused by a distribution of silica species rather than by relaxation effects. That silica distribution turns out to be the cause for line broadening has been demonstrated with our spin-echo experiments.

Compared to crystalline SiO_2 phases, the calculated range of ⟨Si–O–Si⟩ values in opals corresponds most closely to that of tridymite MC, i.e., tridymite with 12 nonequivalent Si positions (Baur, 1977). For tridymite MC, the average chemical shift is -111 ppm (Smith and Blackwell, 1983) with a corresponding ⟨Si–O–Si⟩ angle of 150°, whereas for tridymite OP, i.e., tridymite with 80

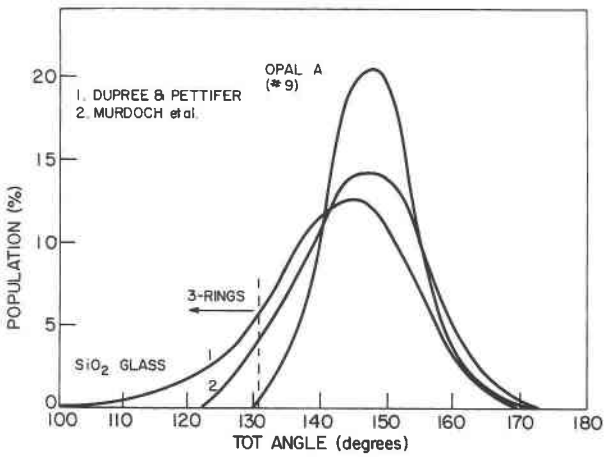

Fig. 4. Comparison between ⟨Si–O–Si⟩ distribution of opal-A and amorphous silica using the formula of Thomas et al. (1983). The sample of Dupree and Pettifer (1984) is most likely silica gel.

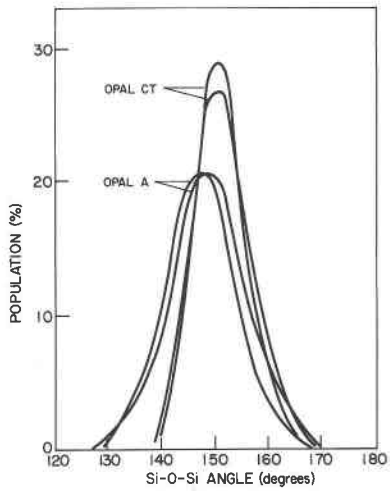

Fig. 5. Variation in ⟨Si–O–Si⟩ distribution between opal-A and opal-CT using the formula of Thomas et al. (1983).

nonequivalent Si positions and ⟨Si–O–Si⟩ angle of 148.3° (Konnert and Appleman, 1978), no NMR spectrum has been measured to date. The maximum and minimum ⟨Si–O–Si⟩ angles observed from X-ray diffraction in tridymite MC are 157.5° and 146.7°, respectively, obviously a range of values substantially narrower than the one observed in opals. The single Si site in cristobalite has a chemical shift of −108.5 ppm corresponding to a ⟨Si–O–Si⟩ of 146.4° (Dollase, 1965). Thus in terms of chemical shifts and variation in ⟨Si–O–Si⟩ distribution, local Si environments in opal most resemble those in tridymite. The major difference is that for opals, the correlation between ⟨Si–O–Si⟩ and ^{29}Si NMR chemical shift indicates the presence of tetrahedra with ⟨Si–O–Si⟩ angles as small as 133°, whereas tridymite contains no such tetrahedra.

It needs to be pointed out that there is a difference between angular distributions obtained from NMR chemical shifts and from X-ray diffraction. The latter technique in its application to amorphous solids assigns angular distributions based upon experimentally determined Si–O, Si–Si, and O–O distances, resulting in a distribution of individual Si–O–Si angles (Taylor and Brown, 1979). On the other hand, NMR measures a distribution of mean Si–O–Si angles, ⟨Si–O–Si⟩, per tetrahedron. These two distributions are not necessarily the same, as can be illustrated for tridymite MC. In this crystal the minimum and maximum ⟨Si–O–Si⟩ angles are 146.7° and 157.5°, respectively, whereas the minimum and maximum Si–O–Si angles are 143.4° and 179.1°, respectively (Baur, 1977).

In addition to the empirical formula derived by Thomas et al. (1983), three other semi-empirical formulas have been constructed to relate chemical shift to ⟨Si–O–Si⟩ angle (Radeglia and Engelhardt, 1985; Ramdas and Klinowski, 1984; Smith and Blackwell, 1983). These three relationships address different facets of variation in the diamagnetic contribution to the chemical shift, focusing attention on electron-density variation on Si (Ramdas and Klinowski, 1984), on oxygen (Radeglia and Engelhardt, 1985), or in the Si–O bond (Smith and Blackwell, 1983). The linear least-squares fits to the data points, correlation coefficients, and chemical-shift cutoff values are collected in Table 2. We have calculated the angular variation for opal sample 9 using these four formulas and illustrate the result in Figure 6. Calculated ⟨Si–O–Si⟩ angular variations using the different formulas are slight except for the relationship of Thomas et al. (1983), which, because it includes in the fitting procedure the chemical shift of zunyite (−128.2 ppm), shifts the Si–O–Si distribution to smaller angles. We have used this last procedure not only because it has the best correlation coefficient (Table 2) but also because it enables calculation of ⟨Si–O–Si⟩ for

TABLE 2. Equations of various least-squares fitted lines used to calculate ⟨Si–O–Si⟩ angles, θ, from ^{29}Si chemical-shift values, δ

Formula (ppm)	Correlation coefficient	Cutoff value of chemical shift (ppm)	Reference* and comments
$\delta = 0.63514 - 241.448(\cos\langle\theta\rangle/(\cos\langle\theta\rangle - 1)$	0.908	120.1	(1) s hybridization of oxygen atoms
$\delta = 149.947 - 270.532(\sin\langle\theta\rangle/2)$	0.910	120.6	(2) non-bonded Si-Si interactions
$\delta = -170.337 - 50.9861(\sec\langle\theta\rangle)$	0.904	119.4	(3) Si-O overlap integrals
$\delta = -19.8215 - 0.608526(\langle\theta\rangle)$	0.911	129.4	(4) empirical

* 1, Radeglia and Engelhardt, 1985; 2, Ramdas and Klinowski, 1984; 3, Smith and Blackwell, 1983; 4, Thomas et al., 1983.

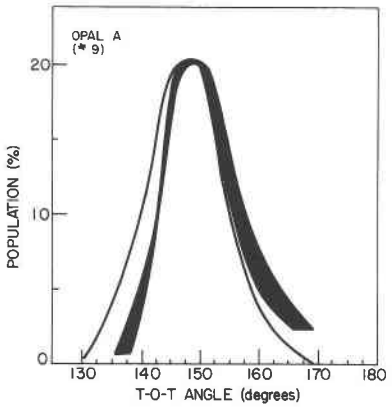

Fig. 6. ⟨Si–O–Si⟩ calculated according to the four formulas collected in Table 2. The single line represents the distribution according to Thomas et al., 1983.

the tail of the opal NMR spectrum that has a chemical shift more negative than −121 ppm.

The ^{29}Si MAS NMR spectrum of a natural opal-CT and the previously published spectra of silica gel, vitreous silica, quartz, tridymite, and cristobalite (Smith and Blackwell, 1983; Murdoch et al., 1985; Maciel and Sindorf, 1980) are shown in Figure 2. Comparison of these spectra clearly indicates that the opal-CT spectrum cannot be constructed by superposition of those of tridymite and cristobalite.

The one synthetic opal measured in this study has a chemical shift of −107 ppm, close to the value for quartz (−107.1 ppm). By analogy with the crystalline silicas, we expected the natural opals, with their chemical shifts around −112 ppm, to be lower in density and refractive index than the synthetic ones. Triplicate measurements of refractive indices and densities of four natural opals and three synthetic ones (two samples manufactured by Inamori and one by Gilson) (Table 3) confirm this hypothesis. Thus, the less-negative chemical shift, i.e., the more quartz-like constitution, of synthetic opals coincides with higher density and higher refractive index. A similar phenomenon is observed in the pressure-induced 16% densification of suprasil, which causes a chemical shift of 2.5 ppm to less-negative values (Devine et al., 1987). The same 16% densification is also observed in neutron irradiation of vitreous silica (Maurer, 1960; Primak, 1958), suggesting that, if pressure and irradiation densification of vitreous silica lead to the same end result, no anomalous Si coordinations occur in either process within NMR detection limits. The chemical-shift variations for amorphous silica species point toward an important feature of NMR spectroscopy, namely, that it can distinguish between amorphous substances that yield similar X-ray diffraction patterns.

Distribution of local Si environments in opal and long-range ordering in opal-CT

Why did we emphasize in the above discussion the similarity or dissimilarity between opal and cristobalite-tridymite? The reason for this is that the X-ray diffraction patterns of opal-CT (Fig. 3) are usually interpreted as being due to disordered cristobalite (Flörke, 1956; Kastner, 1979; Graetsch et al., 1987). Thus from the X-ray evidence one might have expected NMR spectra of opals with chemical shifts around −108 ppm, corresponding to a ⟨Si–O–Si⟩ distribution with a maximum frequency around 146° and a narrower variation in angles than actually observed.

TABLE 3. Density and refractive index of natural and synthetic opals

Sample	Density (g/cm³)	Refractive index
R 12715*	2.129	1.447
R 11399*	2.121	1.448
R 13779*	2.122	1.443
R 11397*	2.122	1.448
R 13154**	2.215	1.460
R 13153**	2.212	1.464
R 13213†	2.209	1.460

* Natural samples.
** Inamori synthetic samples.
† Gilson synthetic sample.

The question arises whether the three peaks in an opal-CT X-ray diffraction pattern were indeed characteristic of disordered cristobalite or whether alternative interpretations are possible. Cristobalite and tridymite both consist of six-membered rings of silica tetrahedra, the ring conformation varying between chairs and boats in tridymite versus chairs only in cristobalite (Taylor and Brown, 1979). The oxygen atoms in crystobalite consist of a three-layer sequence equivalent to the sequence of cubic closest packing, whereas those in tridymite consists of a two-layer sequence equivalent to hexagonal closest packing (Graetsch et al., 1987).

More important as a clue to interpret the opal-CT X-ray diffraction pattern are the characteristic radial distribution maxima for vitreous silica as a function of Si–O–Si angle (Taylor and Brown, 1979). These data indicate that amorphous SiO_2 with straight Si–O–Si angles should have maxima around 1.6, 2.3, and 3.2 Å plus three additional maxima between 3.3 and 4.5 Å (Fig. 7A). Si–O–Si bending causes third- and fourth-nearest-neighbor distances to coincide with maxima around 2.6, 3.5, and 4 Å (Fig. 7B). Comparison of these distances with those observed in opal-CT X-ray patterns indicates that the 4.3-, 4.1-, and 2.5-Å spacings are characteristic oxygen–oxygen distances in angle-constrained silicas. It is therefore equivocal to interpret the opal-CT diffraction pattern as that of disordered cristobalite, ordered cristobalite with a tridymite stacking sequence, or a well-ordered, possibly tridymite-like oxygen array, with cristobalite stacking faults. Any of these stacking sequences, and possibly many more, may give rise to long-range unidirectional ordering of close-packed oxygen atoms, while maintaining local Si environments between those encountered in tridymite and amorphous silica.

The pronounced character of the (101) X-ray diffrac-

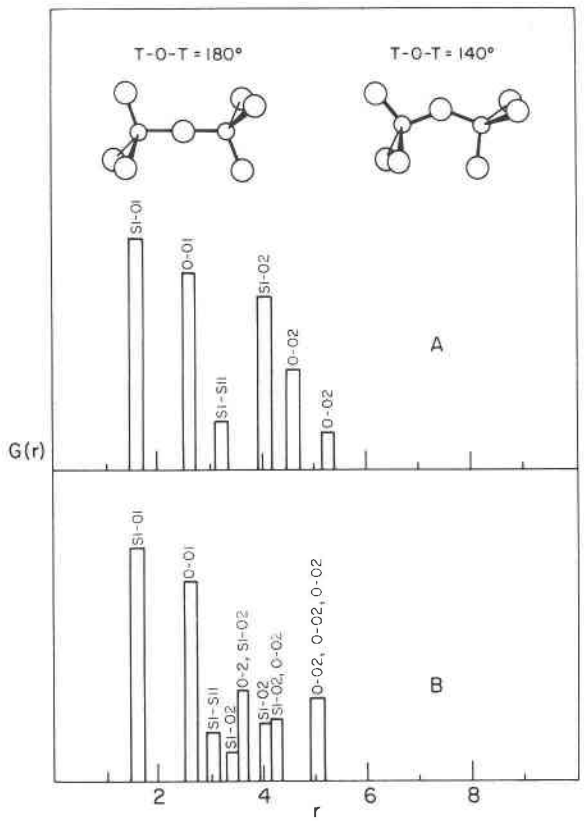

Fig. 7. (A) Distance frequencies in SiO_2 at Si–O–Si angle of 180°. (B) Distance frequencies in SiO_2 at Si–O–Si angle of 140° (Taylor and Brown, 1979).

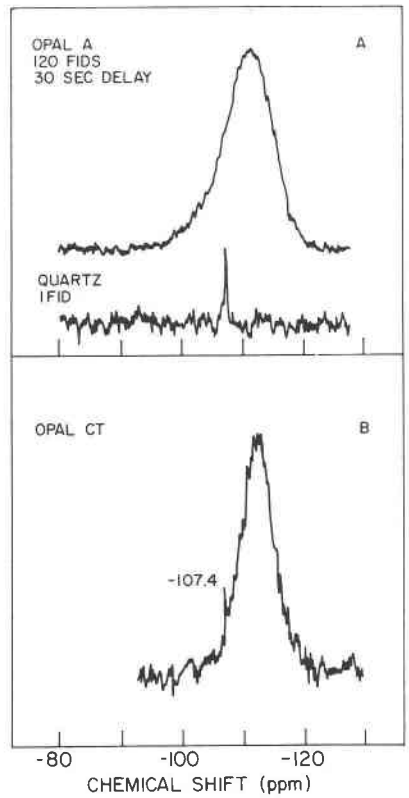

Fig. 8. (A) ^{29}Si MAS NMR spectrum of opal-A and quartz taken with 30-s time interval between pulses. (B) ^{29}Si MAS NMR spectrum of opal-CT taken with 1-h time interval between pulses.

tion peak of opal-CT, sampling long-range ordering of at least 50 Å, and the broad opal-CT ^{29}Si MAS NMR spectrum, resembling amorphous silica much more than tridymite or cristobalite, suggest that in silica species, solid-state transitions are initiated by an ordering of the oxygen array followed by that of the Si sites.

Sensitivity of ^{29}Si MAS NMR vis-à-vis X-ray diffraction in detecting crystalline phases

The preceding section has raised some questions about the common interpretation of X-ray diffraction patterns of opal-CT as indicating the coexistence of microcrystalline and amorphous silica. We address in this section factors pertinent to detecting small amounts of crystalline phases in amorphous silica.

In a two-phase system, as opal-CT is according to X-ray diffraction, detectability of a phase by means of NMR spectroscopy depends on the relative concentration of the phases, whether the peaks overlap, and on the spin-lattice relaxation time, T_1. T_1 values for opal and quartz are about 10 s and 5 h, respectively. Thus, considering only T_1 variations, for a sample of opal-A containing quartz, a 30-s delay between pulses enhances the amorphous component by a factor of 600 relative to quartz.

To determine the conditions under which a small amount of quartz can be detected in opal-A, two experiments were carried out. In the first experiment (Fig. 8A) a ^{29}Si MAS NMR spectrum of quartz was compared with that of sample 6, a quartz-containing opal-A (experimental conditions: 59.6 MHz, 30-s delay, similar spin concentrations). One free-induction decay (FID) of quartz yields a signal to noise (S/N) ratio of three; 120 FIDs of quartz should give a S/N ratio of 33 ($3 \times \sqrt{120}$). Hence if 1/33 or 3% of sample 6 consists of quartz, a peak should appear at −107.4 ppm with a S/N ratio of 1, provided T_1 of quartz in opal is similar to T_1 in quartz alone. The 5% quartz found in the X-ray diffraction pattern of sample 6 does not give rise to a discernible quartz peak in the ^{29}Si MAS NMR spectrum of this sample.

In a second experiment the recycle delay of opal-CT (sample 3) was changed from 30 s to 1 h in order to test for the possibility that cristobalite in this sample has considerably longer T_1 than opal itself. The spectrum did not change except for a very small peak, just above background at −107.4 ppm, characteristic for quartz (Fig. 8B). We conclude from these experiments that, provided that the T_1 of cristobalite is not pathologically long, the local Si environments, sampled by NMR on the scale of 5–6 Å, reflect an arrangement comparable to that of amorphous silica. On the other hand and as already pointed out,

long-range order of at least 50 Å, when sampled by X-ray diffraction, shows a transition toward a crystalline array.

In this context it is of interest to note that oxygen interactions determine geometry in silica species, as demonstrated by de Jong and Brown (1980) and used by Thattachari and Tiller (1982) in modeling the structure of amorphous silica. The data in this study on opals suggest that long-range ordering of the oxygen array has already taken place in opal-CT, whereas the Si atoms have not yet found their equilibrium positions. It is a matter of speculation if such long-range order preceding settlement of local Si environments is the rule rather than the exception in solid-phase transitions from amorphous to crystalline silicates.

Summary and conclusions

Opal-A and opal-CT yield relatively broad ^{29}Si MAS NMR spectra that cannot be interpreted as being due to a superposition of the spectra of crystalline silicas. The X-ray diffraction pattern of opal-CT can therefore not be interpreted as being caused by line broadening due to cristabolite-tridymite microcrystallites for which NMR spectroscopy, sampling local environments in the order of 5 to 6 Å, would show a combination of tridymite and cristobalite peaks. The difference between the X-ray and MAS NMR signatures of opal-A with quartz indicates the greater sensitivity of the former technique to the presence of crystalline phases in this particular system in contrast to, for instance, the detection of corundum in aluminosilicate glasses (de Jong et al., 1983). Results presented here also indicate that long-range ordering in the transition from amorphous to quasi-crystalline opals precedes short-range ordering.

Proton NMR does not indicate a significant amount of silanol groups in opals. Our work suggests the presence of water physisorbed on the substrate, akin to the type of water present in zeolites. Synthetic opals are, according to their ^{29}Si chemical shift, intrinsically more quartz-like than natural ones. As a consequence, such opals can readily be distinguished from natural ones by their higher refractive index and density. Our results indicate, thus, that NMR distinguishes between X-ray-comparable amorphous phases.

Acknowledgments

Water analyses, X-ray diffraction, density, and refractive index measurements were carried out by Vincent van der Mee and Willie van Wesel at Smitweld, the Netherlands, and by Pat Gray at the Gemmological Institute of America, U.S.A. Critical reviews by John Higgins and Jim Kirkpatrick have helped considerably in straightening out the interpretation of the observed phenomena.

References cited

Aujla, R.S., Leng-Ward, G., Lewis, M.H., Seymour, E.F.W., Styles, G.A., and West, G.W. (1986) An NMR study of silicon coordination in Y-Si-Al-O-N glasses. Philosophical Magazine, B54, L51-L56.

Baur, W.H. (1977) Silicon-oxygen bond lengths, bridging angles Si–O–Si and synthetic low tridymite. Acta Crystallographica, B33, 2615–2619.

Deelman, J.C. (1986) Opal-CT in bamboo. Neues Jahrbuch für Mineralogie Monatshefte, 407–415.

de Jong, B.H.W.S., and Brown, G.E. (1980) Polymerization of silicate and aluminate tetrahedra in glasses, melts, and aqueous solutions—I. Electronic structure of $H_6Si_2O_7$, $H_6AlSiO_7^-$, and $H_6Al_2O_7^{2-}$. Geochimica et Cosmochimica Acta, 44, 491–513.

de Jong, B.H.W.S., and Veeman, W.S. (1986) ^{29}Si MAS and ^{23}Na nutation NMR reveal that local sodium environment is principal difference between sodium silicate gel and glass. International Mineralogical Association, Abstracts with Program, 87.

de Jong, B.H.W.S., Keefer, K.D., Brown, G.E., and Taylor, Ch.M. (1981) Polymerization of silicate and aluminate tetrahedra in glasses, melts, and aqueous solutions—III. Local silicon environments and internal nucleation in silicate glasses. Geochimica et Cosmochimica Acta, 45, 1291–1308.

de Jong, B.H.W.S., Schramm, C.M., and Parziale, V.E. (1983) Polymerization of silicate and aluminate tetrahedra in glasses, melts, and aqueous solutions—IV. Aluminum coordination in glasses and aqueous solutions and comments on the aluminum avoidance principle. Geochimica et Cosmochimica Acta, 47, 1223–1237.

——— (1984a) Polymerization of silicate and aluminate tetrahedra in glasses, melts, and aqueous solutions—V. The polymeric structure of silica in albite and anorthite composition glass and the devitrification of amorphous anorthite. Geochimica et Cosmochimica Acta, 48, 2619–2629.

——— (1984b) ^{29}Si magic angle spinning NMR study on local silicon environments in amorphous and crystalline lithium silicates. American Chemical Society Journal, 106, 4396–4402.

Devine, R.A.B., Dupree, R., Farnan, I., and Capponi, J.J. (1987) Pressure-induced bond-angle variation in amorphous SiO_2. Physical Review, B35, 2560–2562.

Dollase, W.A. (1965) Reinvestigation of the structure of low cristobalite. Zeitschrift für Kristallographie, 121, 369–377.

Dupree, R., and Pettifer, R.F. (1984) Determination of the Si–O–Si bond angle distribution in vitreous silica by magic angle spinning NMR. Nature, 308, 523–525.

Dupree, R., Holland, D., McMillan, P.W., and Pettifer, R.F. (1984) The structure of soda-silicate glasses: A MAS NMR study. Journal of Non-Crystalline Solids, 68, 399–410.

Dupree, R., Holland, D., and Williams, D.S. (1986) The structure of binary alkali silicate glasses. Journal of Non-Crystalline Solids, 81, 185–200.

Engelhardt, G., Nofz, M., Forkel, K., Wihsmann, F.G., Mägi, M., Samoson, A., and Lippmaa, E. (1985) Structural studies of calcium aluminosilicate glasses by high resolution solid state ^{29}Si and ^{27}Al magic angle spinning nuclear magnetic resonance. Physics and Chemistry of Glasses, 26, 157–165.

Fagherazzi, H.P., Zardetto, G., and Raiteri, F. (1981) X-ray line broadening Fourier analysis. II. Application to a glass-ceramic system and to copper filings. Gazetta Chimica Italia, 111, 137–143.

Flörke, O.W. (1956) Zur frage des "hoch"-cristobalit in opalen bentoniten und gläsern. Neues Jahrbuch für Mineralogie Monatshefte, 217–223.

Frondel, C. (1962) The system of mineralogy, vol. III, 334 p. Wiley, New York.

Fujiu, T., and Ogino, M. (1984) ^{29}Si NMR study on the structure of lead-silicate glasses. Journal of Non-Crystalline Solids, 64, 287–290.

Garofalini, S.H. (1984) Defect species in vitreous silica—A molecular dynamics simulation. Journal of Non-Crystalline Solids, 63, 337–345.

Gauthier, J.P. (1985) Direct observation of different types of opal by transmission electron microscopy: I. Gem opal. Journal de Microscopie et Spectroscopie Electronique, 10, 117–128.

——— (1986) Synthèse et imitation de l'opal noble. Revue de Gemmologie A.F.G., 89, 16–23.

Gerstein, B.C., and Nicol, A.T. (1985) Crystallinity and local chemical environments of silicon in a silicon-aluminum-oxygen glass ceramic. Journal of Non-Crystalline Solids, 75, 423–428.

Gladden, L.F., Carpenter, T.A., and Elliott, S.R. (1986) ^{29}Si MASNMR studies of the spin-lattice relaxation time and bond-angle distribution in vitreous silica. Philosophical Magazine, B53, L81–L87.

Graetsch, H., Flörke, O.W., and Miehe, G. (1985) The nature of water in chalcedony and opal-C from Brazilian agate geodes. Physics and Chemistry of Minerals, 12, 300–306.

——— (1987) Structural defects in microcrystalline silica. Physics and Chemistry of Minerals, 14, 249–257.

Grimmer, A.R., Mägi, M., Hähnert, M., Stade, H., Samoson, A., Weiker, W., and Lippmaa, E. (1984) High resolution solid state ^{29}Si nuclear magnetic resonance spectroscopic studies of binary alkali silicate glasses. Physics and Chemistry of Glasses, 25, 105–109.

Hahn, E.L. (1950) Spin echoes. Physical Review, 80, 580–594.

Iler, R.K. (1979) The chemistry of silica. Wiley, New York, 866 p.

Kano, K. (1983) Ordering of opal-CT in diagenesis. Geochemical Journal, 17, 87–93.

Kastner, M. (1979) Silica polymorphs. Mineralogical Society of America Reviews in Mineralogy, 6, 99–109.

Kirkpatrick, R.J., Smith, K.A., Schramm, S., Turner, G., and Yang, W.H. (1985) Solid state magnetic resonance spectroscopy of minerals. Annual Reviews of Earth and Planetary Sciences, 13, 29–47.

Kirkpatrick, R.J., Oestrike, R., Weiss, C.A., Smith, K.A., and Oldfield, E. (1986) High-resolution ^{27}Al and ^{29}Si NMR spectroscopy of glasses and crystals along the join $CaMgSi_2O_6$-$CaAl_2SiO_6$. American Mineralogist, 71, 705–711.

Klinowski, J. (1984) Nuclear magnetic resonance studies of zeolites. Progress in NMR Spectroscopy, 16, 237–309.

Klug, H.P., and Alexander, L.E. (1954) X-ray diffraction procedures. Wiley, New York, 716 p.

Knauth, L.P., and Epstein, S. (1982) The nature of water in hydrous silica. American Mineralogist, 67, 510–520.

Konnert, J.H., and Appleman, D.E. (1978) The crystal structure of low tridymite. Acta Crystallographica, B34, 391–403.

Lippmaa, E., Mägi, M., Samoson, A., Engelhardt, G., and Grimmer, A.R. (1980) Structural studies of silicates by solid-state high-resolution ^{29}Si NMR. American Chemical Society Journal, 102, 4889–4893.

Maciel, G.E., and Sindorf, D.W. (1980) Silicon-29 nuclear magnetic resonance study of the surface of silica gel by cross polarization and magic-angle spinning. American Chemical Society Journal, 102, 7606–7607.

Matson, D.W., Sharma, S.K., and Philpotts, J.A. (1983) The structure of high silica alkali-silicate glasses: A Raman spectroscopic investigation. Journal of Non-Crystalline Solids, 58, 323–352.

Maurer, R.D. (1960) Light scattering by neutron irradiated silica. International Journal of Physics and Chemistry of Solids, 17, 44–51.

Murata, K.J., and Nakata, J.K. (1974) Cristobalite stage in the diagenesis of diatomaceous shale. Science, 184, 567–568.

Murdoch, J.B., Stebbins, J.F., and Carmichael, I.S.E. (1985) High resolution ^{29}Si NMR study of silicate and aluminosilicate glasses: The affect of network modifying cations. American Mineralogist, 70, 332–343.

Nukui, A., and Flörke, O.W. (1987) Three tridymite structural modifications and cristobalite intergrown in one crystal. American Mineralogist, 72, 167–169.

O'Keeffe, M., and Gibbs, G.V. (1984) Defects in amorphous silica: Ab initio calculations. Journal of Chemical Physics, 81, 876–879.

Oldfield, E., and Kirkpatrick, R.J. (1984) High resolution magnetic resonance of inorganic solids. Science, 227, 1537–1544.

Phillips, J.C. (1980) Chemical bonding, internal surfaces, and the topology of noncrystalline solids. Physica Status Solidi, B101, 473–479.

Primak, W. (1958) Fast-neutron-induced changes in quartz and vitreous silica. Physical Review, 110, 1240–1254.

Radeglia, R., and Engelhardt, G. (1985) Correlation of Si–O–T (T = Si or Al) and ^{29}Si NMR chemical shifts in silicates and aluminosilicates. Interpretation by semi-empirical quantum-chemical considerations. Chemical Physics Letters, 114, 28–30.

Ramdas, S., and Klinowski, J. (1984) A simple correlation between isotropic ^{29}Si chemical shifts and T–O–T angles in zeolite frameworks. Nature, 308, 521–523.

Sanders, J.V. (1985) Structure of opals. Journal de Physique, 46, C3, 1–C3, 8.

Schneider, E., Stebbins, J.F., and Pines, A. (1987) Speciation and local structure in alkali and alkaline earth silicate glasses: Constraints from ^{29}Si NMR spectroscopy. Journal of Non-Crystalline Solids, 89, 371–383.

Simonton, T.C., Roy, R., Komarneni, S., and Breval, E. (1986) Microstructure and mechanical properties of synthetic opal: A chemically bonded ceramic. Journal of Materials Research, 1, 667–674.

Smith, J.V., and Blackwell, C.S. (1983) Nuclear magnetic resonance of silica polymorphs. Nature, 303, 223–225.

Stebbins, J.F., Murdoch, J.B., Schneider, E., Carmichael, I.S.E., and Pines, A. (1985) A high temperature high-resolution NMR study of ^{23}Na, ^{27}Al, and ^{29}Si in molten silicates. Nature, 314, 250–252.

Taylor, M., and Brown, G.E. (1979) Structure of mineral glasses—I. The feldspar glasses $NaAlSi_3O_8$, $KAlSi_3O_8$, $CaAl_2Si_2O_8$. Geochemica et Cosmochimica Acta, 43, 61–75.

Thattachari, Y.T., and Tiller, W.A. (1982) Steric factors in the spatial structure of silicas. In R. Srinivasan and R.H. Sarma, Eds., Conformation in biology, p. 445–452. Adenine Press, New York.

Thomas, J.M., Klinowski, J., Ramdas, S., Hunter, B.K., and Tennakoon, D.T.B. (1983) The evaluation of nonequivalent tetrahedral sites from silicon-29 NMR chemical shifts in zeolites and related aluminosilicates. Chemical Physics Letters, 102, 158–162.

Turner, G.L., Kirkpatrick, R.J., Risbud, S.H., and Oldfield, E. (1987) Multinuclear magic-angle simple-spinning nuclear magnetic resonance spectroscopic studies of crystalline and amorphous ceramic materials. American Ceramic Society Bulletin, 66, 656–663.

Vieillard, P. (1986) Relation entre structure et parametres thermodynamiques des phases de la silica. Bulletin de Minéralogie, 109, 219–238.

Weeding, T.L., de Jong, B.H.W.S., Veeman, W.S., and Aitken, B.G. (1985) Silicon coordination changes from 4-fold to 6-fold on devitrification of silicon phosphate glass. Nature, 318, 352–353.

Weyl, W.A., and Marboe, E.Ch. (1959) Structural changes during melting of crystals and glasses. Journal of the Society of Glass Technology, 43, 417–437.

Yang, W.H., Kirkpatrick, R.J., and Turner, G. (1986) ^{31}P and ^{29}Si MASNMR investigation of the structural environments of phosphorus in alkaline-earth silicate glasses. American Ceramic Society Journal, 69, C222–223.

MANUSCRIPT RECEIVED DECEMBER 18, 1986
MANUSCRIPT ACCEPTED JULY 14, 1987